

Magnetic Phase Separation in $\text{La}_{1-x}\text{Sr}_x\text{CoO}_3$ by ^{59}Co Nuclear Magnetic Resonance

P. L. Kuhns,¹ M. J. R. Hoch,¹ W. G. Moulton,¹ A. P. Reyes,¹ J. Wu,² and C. Leighton²

¹National High Magnetic Field Laboratory, Tallahassee, Florida 32310, USA

²Department of Chemical Engineering and Materials Science, University of Minnesota, Minneapolis, Minnesota 55455, USA

(Received 21 January 2003; published 16 September 2003)

^{59}Co NMR measurements on $\text{La}_{1-x}\text{Sr}_x\text{CoO}_3$ reported here establish unequivocally, for the first time, the coexistence of ferromagnetic regions, spin-glass regions, and hole-poor low spin regions at all x values from 0.1 to 0.5. A zero external field NMR spectrum, which is assigned to the ferromagnetic regions, has a spectral shape that is nearly x independent at 1.9 K, as are the relaxation times, T_1 and T_2 . The integrated spectral area increases rapidly with x up to $x = 0.2$ and then decreases slightly for larger x . In a field of 9.97 T, a narrow NMR line is observed at 102 MHz, identical to that found in $x = 0$ samples in previous work. The integrated intensity of this spectrum decreases rapidly with increasing x , and is ascribed to hole-poor low spin regions. Beneath this spectrum, a third broad line, with a peak at 100 MHz, is assigned to a spin- or cluster-glass-like phase.

DOI: 10.1103/PhysRevLett.91.127202

PACS numbers: 75.30.Kz, 75.50.Cc, 76.60.Jx

Intrinsic inhomogeneities play a crucial role in the unusual magnetoelectronic properties of doped perovskites including manganites and cuprates [1]. It is likely that magnetic phase separation is at least as important in the cobaltites as in other oxides, as evidenced by the unusual magnetic properties of doped cobaltites which are interpreted in terms of magnetic clusters [2]. The present work is directed toward identifying and investigating such phase separation in $\text{La}_{1-x}\text{Sr}_x\text{CoO}_3$ using NMR as a microscopic probe. The magnetic and transport properties of the doped perovskite systems $\text{La}_{1-x}\text{Sr}_x\text{MO}_3$ ($M = \text{Mn}$ or Co) have attracted considerable recent attention [1–4]. Hole doping by substitution of a divalent ion for La induces a metal-insulator (MI) transition together with ferromagnetism (FM), while double exchange, involving Mn or Co ions in different charge states, provides the FM coupling mechanism.

Magnetic and electrical transport measurements on $\text{La}_{1-x}\text{Sr}_x\text{CoO}_3$ (LSCO) have revealed spin-glass (SG) properties, large magnetoresistance, and giant anomalous Hall effects which are not well understood [5–7]. A recently proposed phase diagram [7], shows paramagnetic, SG, and ferromagnetic cluster glass (CG) regions with the low temperature SG to FM CG change occurring at $x = 0.18$, coincident with a MI transition. For Sr concentrations in the range $0.2 < x < 0.5$, the transition temperature, T_c , to a FM phase is weakly x dependent and approximately 240 K. The CG magnetic properties include memory effects characteristic of glassy systems [8–11]. LSCO has a rhombohedrally distorted perovskite structure that is close to cubic [2]. Recent experimental [7] and theoretical work [12] suggests that both Co^{3+} and Co^{4+} ions are in the intermediate spin state (IS) $t_{2g}^5 e_g^1$ for Co^{3+} and $t_{2g}^4 e_g^1$ for Co^{4+} . There is evidence of a small distortion [2,13] of the oxygen octahedron, involving changes in the Co-O bond angle near the ordering temperature for $x \geq 0.1$. Neutron data show that local dy-

namic Jahn-Teller (JT) distortions [13] stabilize the IS state. Small changes in covalent hybridization of Co d and O p states can produce large changes in properties. In this mixed valence system, double exchange between the Co^{3+} and Co^{4+} gives rise to FM coupling, while exchange between like ions produces antiferromagnetic (AFM) coupling. Long range interactions between JT sites can lead to frustration and SG behavior [13] different from frustrated short-range interactions. The MI transition occurs when the percolation threshold of FM clusters is reached, and is coincident with the onset of FM-like behavior in the bulk magnetic properties.

Efforts are under way to understand the mechanisms of magnetic phase separation [14]. In the well-studied manganites [14], neutron diffraction [15], scanning tunneling microscopy [16], noise measurements [17], and NMR [18,19] have been used to probe magnetic phase separation, while x-ray absorption fine structure [20] has revealed a possible structural precursor. For LSCO, high-resolution transmission electron microscopy has revealed an inhomogeneous distribution of Sr-rich and La-rich regions [2] with sizes 8 to 40 nm. Neutron diffraction experiments [2] show that the low temperature FM correlation length is several hundred angstroms, while small-angle-neutron-scattering (SANS) [2] shows magnetic clustering effects, on a scale of 10 to 15 Å.

There have been only a few previous NMR publications on the cobaltites. Low field continuous wave NMR (8 MHz) ^{59}Co measurements by Bose *et al.* [21] gave a quadrupole coupling constant, $\nu_Q = 0.6$ MHz with axial symmetry ($\eta = 0$). Later ^{59}Co spin echo NMR experiments on $\text{La}_{1-x}\text{Sr}_x\text{CoO}_3$ ($x \leq 0.15$) confirmed this ν_Q value [22] and ^{59}Co NMR lines were observed for $x \leq 0.08$. A broad zero field spectrum, observed for $x \geq 0.2$ and $T = 4.2$ K, was interpreted in terms of FM regions. Kobayashi *et al.* [23] have recently made ^{59}Co spin echo measurements at 95.0 MHz on single crystals of LaCoO_3

and $\text{La}_{0.95}\text{Sr}_{0.05}\text{CoO}_3$, with results which are consistent with the earlier work, and also observed a low spin state spectrum in the 0.05 sample.

In our experiments, both zero field and high field ^{59}Co NMR have been employed to obtain information on the microstructure and magnetic phase separation of LSCO over a wide x range. The samples were prepared by solid-state reaction at 980°C followed by cold pressing, sintering for 24 h at 1350°C , and slow cooling. Characterization using x-ray diffraction, scanning electron microscopy, iodometric titration, and spatially resolved (micron scale) energy dispersive x-ray spectroscopy showed that the material is stoichiometric and uniform within the resolution, with grain sizes of a few microns [7].

Spin echo NMR measurements were made using a computer controlled wide-band spectrometer with an untuned low temperature probe. Spin echo signals were observed either in zero field or in fields up to 10 T. The spectrometer response and calibration were carried out at 10 MHz intervals over the range 40–250 MHz using a ^7Li NMR signal at 2 K, and all data were corrected using this response curve. This procedure takes into account probe and spectrometer frequency response, which typically varies by a factor of 2 or more over this large frequency range, and includes the $1/f^2$ correction automatically. No measurable differences in the spectra were found for field cooled or zero field cooled protocols. The signal was monitored during cooldown (300–1.9 K), with cool down times ranging from 16 h to less than 10 min. The time to reach maximum signal amplitude after reaching base temperature, 1.9 K, was hours for slow cooling and 30 min for fast cooling. This suggests some cooperative expansion of the FM regions following cooling. It is important to note the signal intensity and integrated area came to the same final value, independent of the cool down rate. All spectra have a broad peak centered at 172 MHz, with unresolved structural features at other frequencies, as shown in Fig. 1. The data have been corrected for the measured spectrometer response and scaled with the molar fraction in each case. For NMR in FM, the rf excitation pulse as well as the signal are enhanced by the hyperfine field within domains, and additionally enhanced within any domain walls. For ^{59}Co NMR, the enhancement factor η was about 40, independent of composition, a low value compared to that found in the FM manganites [24]. The spectral shape is relatively independent of x , but with a small increase in the spectral component centered at 120 MHz, as x is increased. Optimal pulse lengths and carefully chosen signal integration limits were used to give the proper line shape. While the spectra are similar in some respects to those obtained by Itoh and Natori [22], our results show smaller changes with x . It is likely that use of the measured spectrometer response in our work, rather than the $1/f^2$ correction, accounts for some of

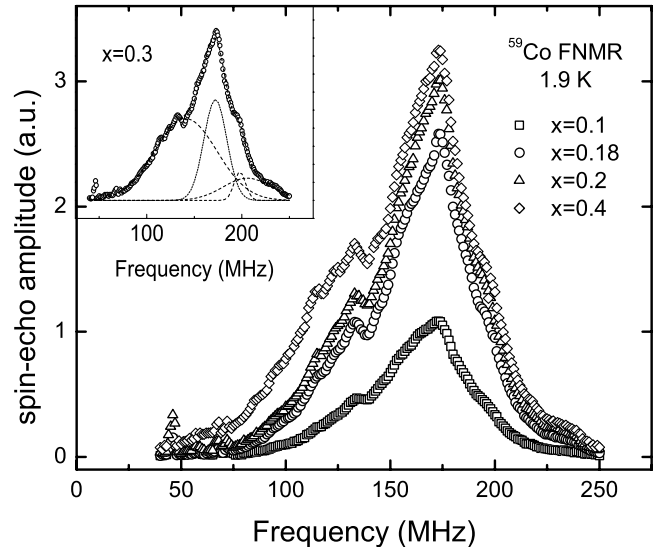


FIG. 1. Zero field ^{59}Co FNMR spectrum for $\text{La}_{1-x}\text{Sr}_x\text{CoO}_3$ for $x = 0.1, 0.18, 0.2,$ and 0.4 . (Inset) Four Gaussian fit of the $x = 0.3$ spectrum. The peaks are at 206, 198, 172, and 142 MHz. The peak positions are independent of x , but the weight of the low frequency peak increases with x at the expense of the two high frequency peaks.

the difference. There is also the possibility of sample differences.

The ZF detection of ferromagnetic NMR (FNMR) for $x < 0.18$ demonstrates that the region denoted SG or CG in the phase diagram [7] contains FM regions below the percolation limit. The Hamiltonian for the system in zero field is

$$\mathcal{H} = \mathcal{H}_{\text{hf}} + \mathcal{H}_Q,$$

where $\mathcal{H}_{\text{hf}} = \mathbf{I} \cdot \mathbf{A} \cdot \mathbf{S}$ is the hyperfine and \mathcal{H}_Q the quadrupolar Hamiltonian, with \mathbf{I} the nuclear spin, and \mathbf{A} the hyperfine coupling tensor including both the isotropic (contact) and the anisotropic parts. The quadrupolar interaction is a small perturbation on \mathcal{H}_{hf} . For spins \mathbf{I} with hyperfine coupling A_i , the resonance frequency is $\nu = \gamma_n A_i \langle S \rangle$, where γ_n is the nuclear magnetogyric ratio and $\langle S \rangle$ the ensemble average electron spin along the principal axis. We assume that the magnetization, $M = Ng\beta \langle S \rangle$, where N is the number of spins, is relatively uniform within the FM regions implying the lineshape can be attributed to a distribution of hyperfine couplings. In the metallic phase ($x > 0.18$) and below the percolation threshold ($0.10 < x < 0.18$), the FM cluster regions are itinerant FM. Double exchange processes on a time scale \hbar/J , where J is the exchange coupling, lead to an averaging of the hyperfine coupling between Co^{3+} and Co^{4+} sites. This gives rise to an averaged spin state for these ions. It is likely that local lattice distortions, due to the random replacement of La ions by larger Sr ions, lead to changes in the d orbitals for adjacent Co ions, producing changes in the core polarization and hence the local

hyperfine coupling, giving a broad range of hyperfine fields. The line shape fit for four Gaussian peaks is shown in Fig. 1. This fitting procedure may well not be unique, but provides an empirical indication of the distribution of hyperfine couplings. The area of the peak centered at 172 MHz is essentially independent of x , while the area of the low frequency (142 MHz) peak increases rapidly with x , possibly reflecting the dependence of the Co hyperfine couplings on the number of nearest neighbor Sr ions and concomitant local distortions. The high frequency (206 MHz) Gaussian component correspondingly decreases with increasing x .

When a magnetic field in the range 0.5 to 5.0 T was applied to the system, the FM peak spectral amplitude observed with short pulses (0.6 μ s), corresponding to the signal with the largest η , showed a rapid decrease with increasing field, although the spectral line shape remained essentially unaltered. For $B = 5.0$ T, the signal amplitude was unobservably weak at $T = 2$ K. The lack of shift with field is reminiscent of the shielding within domain walls in a conventional FM. Using longer pulses (5 μ s), weak echo signals were observed with a shift of the spectrum to higher frequencies with increasing field corresponding to the hyperfine field acting parallel to the magnetization direction, in contrast with the usual shift to lower frequencies found in other FM cobalt systems. Further work is needed to understand the behavior of the FM component of the system in applied fields.

Spin echo NMR experiments were carried out at temperatures down to 1.9 K in an applied field of 9.97 T, for which the unshifted ^{59}Co Larmor frequency is 100 MHz. Above 15 K the signal is not observable even with 10^4 scans. Spectra are shown in Fig. 2 for various x values in

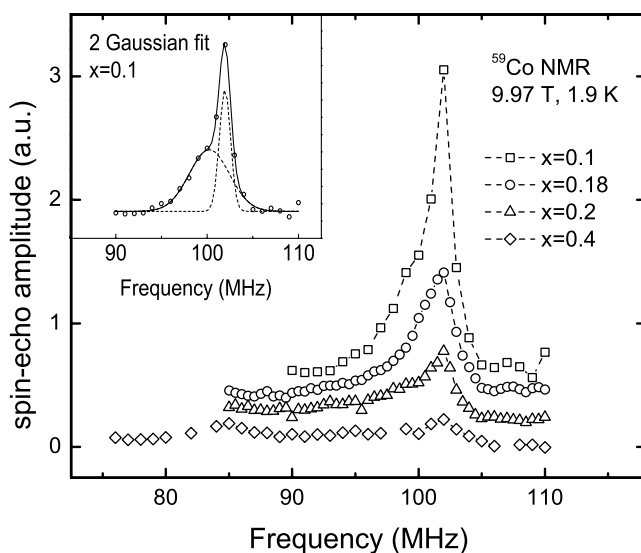


FIG. 2. ^{59}Co NMR spectra in a field of $B = 9.97$ T for Sr concentrations x in the range 0.1 to 0.4. The fitted Gaussian curves for $x = 0.1$ (inset) are centered at 100 MHz and 102 MHz, respectively. The baselines are offset for clarity.

the range 0.1 to 0.4. This is in contrast to previous work [22] which found no NMR corresponding to the low spin state above $x = 0.15$. All spectra have two main components, a narrow line centered at 102 MHz, with the same Knight shift as in LaCoO_3 plus a broad component with a peak at 100 MHz and a long low frequency tail, extending over more than 10 MHz. Both components, with enhancement factor near 1, decrease with increasing x , with the broad 100 MHz component becoming relatively more prominent. The narrow 102 MHz spectrum is assigned to hole-poor low spin regions, given the similarity to data on $x = 0$ samples [22]. A two Gaussian fit is shown in the inset of Fig. 2. For the 102 MHz signal, the relaxation time T_1 is 820 ms and T_2 is 247 ms at 2 K, independent of x , close to the values for LaCoO_3 [23]. T_1 at 98 MHz (assigned to the glass phase) is 22 ms at 2 K, clearly indicating magnetic relaxation and a different phase. The T_1 recovery curves for both broad and narrow signals require a stretched exponential fit indicating a distribution of relaxation times. The broad signal is assigned to the spin-glass-like region, which is thought to contain both LS and IS components. JT distortions have been shown to be important in this phase [13]. Such effects may give rise to dynamically fluctuating spin polarons [2,25], composite structures with a hole, or holes, distributed over a number of adjacent Co sites, which become increasingly important at temperatures approaching T_c . The long spectral tail below 100 MHz is consistent with a distribution of hyperfine fields in the non-FM region. T_2 is single exponential. The ^{59}Co Knight shift in undoped $x = 0$ and $x = 0.05$ LaCoO_3 samples is $\langle K \rangle = 2\%$, attributed to Van Vleck orbital paramagnetism for Co ions in the LS ($S = 0$) state [22]. On this basis, along with the long relaxation times, it is concluded the 102 MHz spectrum arises from ions in the LS Co^{III} state in hole-poor regions, possibly of very low Sr concentration. The results show that a number of LS ions persist in samples with

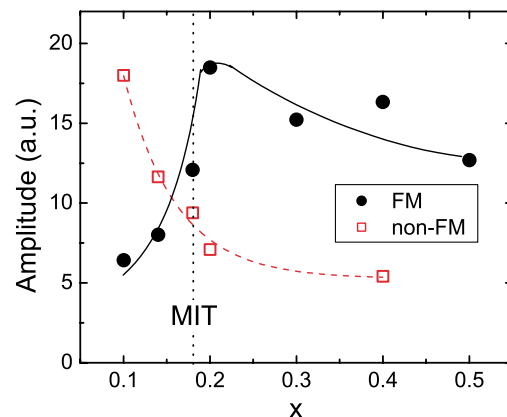


FIG. 3 (color online). The total integrated area of the zero field spectra and the narrow, 102 MHz Gaussian LS 9.97T NMR spectra as a function of x , showing the coexistence of the FM and non-FM regions over the entire range of composition.

x values as high as 0.5. It has been reported that annealing at $\geq 1200^\circ\text{C}$ suppresses this phase [26]. However, these samples were annealed at 1350°C , and the low spin phase is clearly present at all x values, suggesting the low spin phase may be intrinsic.

Figure 3 shows total areas of the ZF spectra, and of the Gaussian fit of the 9.97 T (102 MHz) NMR spectra, as a function of x . These areas are proportional to the number of Co spins in FM and in non-FM, LS regions, respectively. There is a marked, continuous, increase in FM area as x increases from 0.1, followed by a slow decrease for $x > x_c$, while the 102 MHz NMR signal decreases rapidly with x but is observable up to $x = 0.5$. The 100 MHz peak decreases in magnitude with x but the poor signal-to-noise ratio for $x > x_c$, together with the evolution of the long tail region, makes determination of the area impractical.

Measurements of T_1 and T_2 as a function of temperature for the FM component in zero field will be reported on in detail elsewhere. The rates $1/T_1$ and $1/T_2$ depend linearly on T and are, within experimental error, independent of Sr concentration. The ratio T_2/T_1 is approximately constant over the temperature range covered, suggesting a common mechanism for the two processes. T_2 becomes so short as T is raised that measurements at temperatures higher than 25 K are not possible. There was no change in T_1 or T_2 in crossing the MI percolation limit. These results show that the FM behavior is not closely coupled to the MI percolation transition in this system. The near independence of the hyperfine coupling, and the relaxation times, on x implies that the FM clusters have essentially the same ordering properties and spin dynamics above and below the MI (percolation) transition. The 102 MHz signals come from the LS rich regions of the samples, since $\langle K \rangle$ is the same as in $x = 0$ samples, η is near 1, and T_1 and T_2 are long indicating little magnetic relaxation. The data of Fig. 3 provide clear and unequivocal evidence for the multiphase character of the material—FM and non-FM regions coexist over the entire composition range studied. As a result of uncertainties in signal enhancement effects and other factors, the number of spins in the FM and non-FM regions cannot be reliably compared. It is, however, clear from the results that, for $x > 0.18$, the ratio of FM to non-FM spins becomes large.

These ^{59}Co NMR measurements clearly establish the inhomogeneous magnetic nature of LSCO, with FM, spin-glass, and LS regions coexisting on both the insulating and metallic sides of the MI transition. Moreover, the data demonstrate that the FM clusters have the same

couplings and spin dynamics, within the time scale of the NMR measurements, above and below the MI (percolation) transition. The large zero field linewidth and single central peak support a single average spin state for the Co ions in FM regions with a large distribution of hyperfine couplings. Taken together with the 102 MHz high field NMR signal amplitude, which decreases with x , the results are consistent with IS and LS states occurring in different, interpenetrating, spatial regions of the samples. The question of whether the $S = 0$ part of the sample arises from Sr poor regions, due to intrinsic chemical or structural phase separation, or from some other mechanism is currently unclear.

Partial support by the National Science Foundation under cooperative agreement No. DMR-0084173 and the State of Florida is gratefully acknowledged.

-
- [1] E. Dagotto, T. Hotta, and A. Moreo, *Phys. Rep.* **344**, 1 (2001).
 - [2] R. Caciuffo *et al.*, *Phys. Rev. B* **59**, 1068 (1999).
 - [3] J. M. D. Coey, M. Viret, and S. von Molnár, *Adv. Phys.* **48**, 167 (1999).
 - [4] S. Jin and T. H. Teifel, *Science* **264**, 413 (1994); Y. Tokura and N. Nagaosa, *Science* **288**, 462 (2000).
 - [5] G. Briceo, H. Chang, X. Sun, P.G. Schultz, and X.-D. Xiang, *Science* **270**, 5234 (1995).
 - [6] M. Itoh *et al.*, *J. Phys. Soc. Jpn.* **63**, 1486 (1994).
 - [7] J. Wu and C. Leighton, *Phys. Rev. B* **67**, 174408 (2003).
 - [8] G. Aeppli, S. M. Shapiro, R. J. Birgeneau, and H. S. Chan, *Phys. Rev. B* **28**, 5160 (1983).
 - [9] H. Maletta and P. Convert, *Phys. Rev. Lett.* **42**, 108 (1979).
 - [10] D. N. H. Nam *et al.*, *Phys. Rev. B* **59**, 4189 (1999).
 - [11] S. Yamaguchi *et al.*, *J. Phys. Soc. Jpn.* **64**, 1885 (1995).
 - [12] P. Ravindran *et al.*, *J. Appl. Phys.* **91**, 291 (2002).
 - [13] D. Louca *et al.*, *Phys. Rev. B* **60**, 10 378 (1999).
 - [14] J. Burgy *et al.*, *Phys. Rev. Lett.* **87**, 277202 (2001).
 - [15] J.W. Lynn *et al.*, *Phys. Rev. Lett.* **76**, 4046 (1996).
 - [16] M. Fath *et al.*, *Science* **285**, 1540 (1999).
 - [17] B. Raquet, *Phys. Rev. Lett.* **84**, 4485 (2000).
 - [18] G. Papavassiliou *et al.*, *Phys. Rev. Lett.* **84**, 761 (2000).
 - [19] M. M. Savosta *et al.*, *Phys. Rev. Lett.* **87**, 137204 (2001).
 - [20] T. Shibusata *et al.*, *Phys. Rev. Lett.* **88**, 207205 (2002).
 - [21] M. Bose *et al.*, *Phys. Rev. B* **26**, 4871 (1982).
 - [22] M. Itoh and I. Natori, *J. Phys. Soc. Jpn.* **64**, 970 (1995).
 - [23] Y. Kobayashi *et al.*, *Phys. Rev. B* **62**, 410 (2000).
 - [24] M. M. Savosta, V. A. Borodin, and P. Novak, *Phys. Rev. B* **59**, 8778 (1999).
 - [25] S. Yamaguchi *et al.*, *Phys. Rev. B* **53**, R2926 (1996).
 - [26] P. S. Anil Kumar, P. A. Joy, and S. K. Date, *J. Appl. Phys.* **83**, 7375 (1998).